A Static Agostic α-CH···M Interaction Observable by NMR Spectroscopy: Synthesis of the Chromium(II) Alkyl $[Cr_2(CH_2SiMe_3)_6]^{2-}$ and Its Conversion to the Unusual "Windowpane" Bis(metallacycle) Complex $[Cr(\kappa^2C,C'\text{-}CH_2SiMe_2CH_2)_2]^{2-}$

Paige M. Morse, Michael D. Spencer, Scott R. Wilson, and Gregory S. Girolami*

School of Chemical Sciences, University of Illinois at Urbana-Champaign, 505 South Mathews Avenue, Urbana, Illinois 61801

Received December 8, 1993®

Alkylation of $CrCl_2(thf)$ with 3 equiv of $LiCH_2SiMe_3$ yields the dinuclear chromium(II) alkyl anion $[Li(thf)_2]_2[Cr_2(CH_2SiMe_3)_6]$. This essentially diamagnetic compound possesses a "bent" Cr–Cr quadruple bond in which two of the six CH_2SiMe_3 ligands bridge the metal–metal bond; each chromium center also bears two terminal CH_2SiMe_3 ligands. NMR spectroscopy clearly indicates that the bridging CH_2SiMe_3 groups engage in agostic Cr···H—C interactions that, somewhat surprisingly, are static on the NMR time scale at −80 °C. Analysis of the NMR line shapes as a function of temperature indicates that the molecule undergoes two different dynamic processes. One process, which has activation parameters of $\Delta H^\ddagger = 10.6 \pm 0.5$ kcal mol^{-1} and $\Delta S^\ddagger = -4 \pm 2$ eu, has been tentatively ascribed to exchange between the terminal and bridging CH_2SiMe_3 ligands; the other process, which has activation parameters of $\Delta H^\ddagger = 14.1 \pm 0.6$ kcal mol^{-1} and $\Delta S^\ddagger = 17 \pm 3$ eu, is ascribed to rotation of the bridging CH_2SiMe_3 ligands about their Cr—C bonds. The latter values give an estimate of the strength of an agostic Cr···H bond. Addition of *N,N,N',N'*-tetramethylethylenediamine (tmed) to $[Li(thf)_2]_2[Cr_2(CH_2SiMe_3)_6]$ results in cleavage of the metal–metal bond and activation of γ-hydrogen atoms of the CH_2SiMe_3 ligands; the unusual bis(metallacycle) compound $[Li(tmed)]_2[Cr(\kappa^2CC'\text{-}CH_2SiMe_2CH_2)_2]$ results. The X-ray crystal structure of this high-spin ($S = 2$) chromium(II) complex shows that it possesses an unusual "windowpane" structure, in which the square-planar chromium center is the common vertex of two metallacyclobutane rings and the lithium cations form close contacts with the carbon atoms of the α-CH_2 groups. Important bond distances and angles: Cr–C = 2.235(3) Å, Li···C = 2.163(6) Å; Si–C = 1.853(3) Å; C–Cr–C(cis) = 79.0(1)°; Li···C–Si = 158.3(2)°; Cr–C–H = 105(2), 137(2)°; Li···C–H = 76(2), 83(2)°; Si–C–H = 109(2), 115(2)°. Crystal data for $C_{20}H_{52}CrLi_2N_4Si_2$ at −75 °C: triclinic, space group $P\bar{1}$, with $a = 7.811(4)$ Å, $b = 10.336(4)$ Å, $c = 10.720(5)$ Å, $\alpha = 95.12(3)°$, $\beta = 110.87(4)°$, $\gamma = 108.58(5)°$, $V = 746(2)$ Å^3, $Z = 1$, $R_F = 0.043$, and $R_{wF} = 0.058$ for 212 variables and 2261 data with $I > 2.58\sigma(I)$.

Introduction

Three-center C–H···M interactions, or "agostic" interactions, are often encountered as structural features in electronically unsaturated transition-metal alkyl complexes.[1-3] Some of the most interesting agostic interactions are those that involve α-hydrogen atoms. Such α-CH···M interactions are known for a variety of transition metals and fall into two principal categories: those in which the alkyl group is a terminal ligand (I) and those in which the alkyl group bridges[4,5] between two metal centers (II).[6,7] Typically, α-agostic alkyl complexes are dynamic; that is, the agostic hydrogen exchanges rapidly on the NMR time scale with other hydrogen atoms that are attached to the

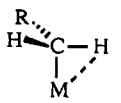

I

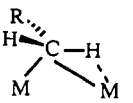

II

α-carbon. With only two exceptions, all known agostic complexes of structure I or structure II have exchange barriers that are sufficiently low so that the NMR spectra are always in the fast-exchange limit.

The two exceptions have structure II, and in both cases, the alkyl groups bridge between two *different* metal atoms; the exchange barrier for rotation of the bridging methyl group in $Cp_2Ti(\mu\text{-}CH_3)(\mu\text{-}CH_2)Rh(cod)$ is 9.8 kcal mol^{-1}, while that for $Cp_2Ti(\mu\text{-}CH_3)(\mu\text{-}CH_2)PtMe(PMePh_2)$ was not reported but is probably similar.[8,9] In one other case of a molecule of structure II, $[Cp_2Fe_2(\mu\text{-}CH_3)(CO)_3]^+$,

® Abstract published in *Advance ACS Abstracts*, April 1, 1994.

(1) Brookhart, M.; Green, M. L. H.; Wong, L.-L. *Prog. Inorg. Chem.* **1988**, *36*, 1–124.

(2) Crabtree, R. H.; Hamilton, D. G. *Adv. Organomet. Chem.* **1988**, *28*, 299–338.

(3) Crabtree, R. H. *Chem. Rev.* **1985**, *85*, 245–269.

(4) Holton, J.; Lappert, M. F.; Pearce, R.; Yarrow, P. I. W. *Chem. Rev.* **1983**, *83*, 135–201.

(5) Casey, C. P.; Audett, J. D. *Chem. Rev.* **1986**, *86*, 339–352.

(6) The metal involved in the agostic interaction is interacting with the α-carbon atom as well, so the designation of the type II structure above as "α-agostic" is reasonable. However, the type II agostic structure can also be thought of as a β-agostic interaction: M–M–C–H.[1]

(7) There is one other structural motif for α-agostic alkyl groups, in which the M···CH_3···M units are nearly linear; such compounds lie outside the scope of the present discussion. See: Waymouth, R. M.; Potter, K. S.; Schaefer, W. P.; Grubbs, R. H. *Organometallics* **1990**, *9*, 2843–2846 and references therein.

(8) Ozawa, F.; Park, J. W.; Mackenzie, P. B.; Schaefer, W. P.; Henling, M. L.; Grubbs, R. H. *J. Am. Chem. Soc.* **1989**, *111*, 1319–1327.

(9) Park, J. W.; Mackenzie, P. B.; Schaefer, W. P.; Grubbs, R. H. *J. Am. Chem. Soc.* **1986**, *108*, 6402–6404.

0276-7333/94/2313-1646$04.50/0

broadening of the NMR resonances at low temperature suggested the onset of a decoalescence process, but a slow-exchange spectrum with distinct signals for the agostic and nonagostic hydrogen atoms could not be attained.[10] There is also an example of a bridging *p*-methylbenzyl ligand which shows distinct resonances for the two α-hydrogen atoms; although the X-ray structure of this complex revealed that one of the two α-hydrogen atoms was agostic, the NMR spectrum is not evidence of a static structure, since the low symmetry of the complex guarantees that the two hydrogen atoms will remain diastereotopic even if rotation of the alkyl group is rapid.[11] A somewhat similar situation pertains for a bridging ethyl group in a dilutetium complex; interestingly, however, exchange of the two diastereotopic α-hydrogen atoms does occur at elevated temperatures, probably via a "linear" μ-alkyl intermediate.[12]

In several thorium alkyls of stoichiometry Cp^*_2ThRR', one of the alkyl groups is involved in two α-agostic interactions with the thorium center, whereas the other alkyl group is normal. Solid-state ^{13}C CPMAS NMR studies have shown that in certain instances exchange of the agostic and nonagostic alkyl groups can be frozen out at low temperatures.[13-15] The dynamic behavior of these complexes differs from that above in that the exchange process involves hydrogens on *different* carbon atoms.

In contrast to the situation for α-agostic hydrogen atoms, there are several examples of compounds in which NMR spectra in the slow-exchange limit can be obtained for agostic interactions that involve hydrogen atoms attached to the β-carbon (or more distant carbon atoms). Among the β-agostic complexes that exhibit static structures by NMR spectroscopy are the ethyl complexes $[CpCoEt(L)]^+$,[16-20] $[Cp^*RhEt(C_2H_4)]^+$,[21] $[NiEt(LL)]^+$,[22] $[PdEt(LL)]^+$,[22] and $[PtEt(LL)]^+$ [23] and the isopropyl complex $(\eta^3\text{-}C_3H_5)Mo(i\text{-}Pr)$.[24] Time-dependent UV–vis absorption studies of $CpW(CO)_2Et$ generated by flash photolysis suggest that the agostic ethyl group is static on the submicrosecond time scale.[25,26] Activation energies for agostic–nonagostic exchange processes have also been measured for certain complexes that contain agostic interactions to more remote hydrogen atoms, although in these cases the ligands involved are not alkyl groups. In virtually all of these molecules, the free energies of activation, $\Delta G^\ddagger$, lie between 8 and 12 kcal mol^{-1}.

Measurements of the strengths of agostic M···H–C interactions have been carried out in a few cases by methods other than NMR spectroscopy. Calorimetric studies of the addition of Lewis bases to the tricyclohexylphosphine complexes $M(CO)_3(PCy_3)_2$ yield an estimate of 10 kcal mol^{-1} for the strength of the agostic interaction with one of the hydrogen atoms of the phosphine ligand.[27-30] Gas-phase infrared and solution photoacoustic and flash photolysis studies of the binding of alkanes to $M(CO)_5$ fragments (M = Cr, Mo, W) demonstrate that the strengths of these interactions are 7–15 kcal mol^{-1}.[31-37] Time-resolved flash photolysis studies have suggested that cyclohexane binds to Cp*Rh(CO) fragments with a similar binding energy.[38] Theoretical calculations of the strengths of various agostic interactions have also been carried out.[39]

We now describe a rare example of an agostic interaction in a complex of structure II that is static on the NMR time scale at low temperatures; this complex is the chromium(II) dimer $[Li(thf)_2]_2[Cr_2(CH_2SiMe_3)_6]$. An analysis of the NMR line shapes as a function of temperature gives activation parameters for interconversion of agostic and nonagostic α-hydrogen atoms. We also describe the conversion of the dinuclear species to an unusual bis(metallacycle) complex via a γ-hydrogen activation process. The resulting bis(metallacycle) compound $[Li(tmed)]_2[Cr(CH_2SiMe_2CH_2)_2]$ has been shown by single-crystal X-ray crystallography to possess an interesting structure consisting of four fused four-membered rings; this complex is an organometallic analogue of the hypothetical organic molecule "windowpane".[40-42]

(10) Casey, C. P.; Fagan, P. J.; Miles, W. H. *J. Am. Chem. Soc.* **1982**, *104*, 1134–1136.
(11) Jeffery, J. C.; Orpen, A. G.; Stone, F. G. A.; Went, M. *J. Chem. Soc., Dalton Trans.* **1986**, 173–186. Note Added in Proof: For other recent examples of this phenomenon, see: Poole, A. D.; Williams, D. N.; Kenwright, A. M.; Gibson, V. C.; Clegg, W.; Hockless, D. C. R.; O'Neil, P. A. *Organometallics* **1993**, *12*, 2549–2555. Etienne, M. *Organometallics* **1994**, *13*, 410–412.
(12) Stern, D.; Sabat, M.; Marks, T. J. *J. Am. Chem. Soc.* **1990**, *112*, 9558–9575.
(13) Bruno, J. W.; Smith, G. M.; Marks, T. J.; Fair, C. K.; Schultz, A. J.; Williams, J. M. *J. Am. Chem. Soc.* **1986**, *108*, 40–56.
(14) Fendrick, C. M.; Schertz, L. D.; Day, V. W.; Marks, T. J. *Organometallics* **1988**, *7*, 1828–1838.
(15) Bruno, J. W.; Marks, T. J.; Day, V. W. *J. Organomet. Chem.* **1983**, *250*, 237–246.
(16) Brookhart, M.; Green, M. L. H.; Pardy, R. B. A. *J. Chem. Soc., Chem. Commun.* **1983**, 691–693.
(17) Cracknell, R. B.; Orpen, A. G.; Spencer, J. L. *J. Chem. Soc., Chem. Commun.* **1984**, 326–328.
(18) Brookhart, M.; Schmidt, G. F.; Lincoln, D.; River, D. S. *Transition Metal Catalyzed Polymerization*; Quirk, R., Ed.; Cambridge University Press: Cambridge, U.K., 1988.
(19) Schmidt, G. F.; Brookhart, M. *J. Am. Chem. Soc.* **1985**, *107*, 1443–1444.
(20) Cracknell, R. B.; Orpen, A. G.; Spencer, J. L. *J. Chem. Soc., Chem. Commun.* **1986**, 1005–1006.
(21) Brookhart, M.; Lincoln, D. M.; Bennett, M. A.; Pelling, S. *J. Am. Chem. Soc.* **1990**, *112*, 2691–2694.
(22) Conroy-Lewis, F. M.; Mole, L.; Redhouse, A. D.; Litster, S. A.; Spencer, J. L. *J. Chem. Soc., Chem. Commun.* **1991**, 1601–1603.
(23) Carr, N.; Mole, L.; Orpen, A. G.; Spencer, J. L. *J. Chem. Soc., Dalton Trans.* **1992**, 2653–2661.
(24) Benn, R.; Holle, S.; Jolly, P. W.; Mynott, R.; Romao, C. C. *Angew. Chem., Int. Ed. Engl.* **1986**, *25*, 555–556.
(25) Kazlaukas, R. J.; Wrighton, M. S. *J. Am. Chem. Soc.* **1982**, *104*, 6005–6015.
(26) Yang, G. K.; Peters, K. S.; Vaida, V. *J. Am. Chem. Soc.* **1986**, *108*, 2511–2513.
(27) Gonzalez, A. A.; Zhang, K.; Nolan, S. P.; de la Vega, R. L.; Mukerjee, S. L.; Hoff, C. D.; Kubas, G. J. *Organometallics* **1988**, *7*, 2429–2435.
(28) Zhang, K.; Gonzalez, A. A.; Hoff, C. D. *J. Am. Chem. Soc.* **1989**, *111*, 3627–3632.
(29) Gonzalez, A. A.; Zhang, K.; Hoff, C. D. *Inorg. Chem.* **1989**, *28*, 4285–4290.
(30) Zhang, K.; Gonzalez, A. A.; Mukerjee, S. L.; Chou, S.-J.; Hoff, C. D.; Kubat-Martin, K. A.; Barnhart, D.; Kubas, G. J. *J. Am. Chem. Soc.* **1991**, *113*, 9170–9176.
(31) Lees, A.; Adamson, A. W. *Inorg. Chem.* **1981**, *20*, 4381–4384.
(32) Yang, G. K.; Peters, K. S.; Vaida, V. *Chem. Phys. Lett.* **1986**, *125*, 566–568.
(33) Ishikawa, Y.; Brown, C. E.; Hackett, P. A.; Rayner, D. M. *Chem. Phys. Lett.* **1988**, *150*, 506–510.
(34) Church, S. P.; Hermann, H.; Grevels, F. W.; Schaffner, K. *Inorg. Chem.* **1988**, *24*, 418–422.
(35) Morse, J. M., Jr.; Parker, G. H.; Burkey, T. J. *Organometallics* **1989**, *8*, 2471–2474.
(36) Brown, C. E.; Ishikawa, Y.; Hackett, P. A.; Rayner, D. M. *J. Am. Chem. Soc.* **1990**, *112*, 2530–2536.
(37) Asali, K. J.; van Zyl, G. J.; Dobson, G. R. *Inorg. Chem.* **1988**, *27*, 3314–3319.
(38) Weiller, B. H.; Wasserman, E. P.; Bergman, R. G.; Moore, C. B.; Pimentel, G. C. *J. Am. Chem. Soc.* **1989**, *111*, 8288–8290.
(39) Saillard, J.-Y.; Hoffmann, R. *J. Am. Chem. Soc.* **1984**, *106*, 2006–2026.
(40) Wiberg, K. B.; Wendoloski, J. J. *J. Am. Chem. Soc.* **1982**, *104*, 5679–5686.
(41) Schulman, J. M.; Sabio, M. L.; Disch, R. L. *J. Am. Chem. Soc.* **1983**, *105*, 743–744.
(42) Rong, G. *Youji Huaxue* **1990**, *10*, 15–25; *Chem. Abstr.* **1991**, *113*, R5729f.

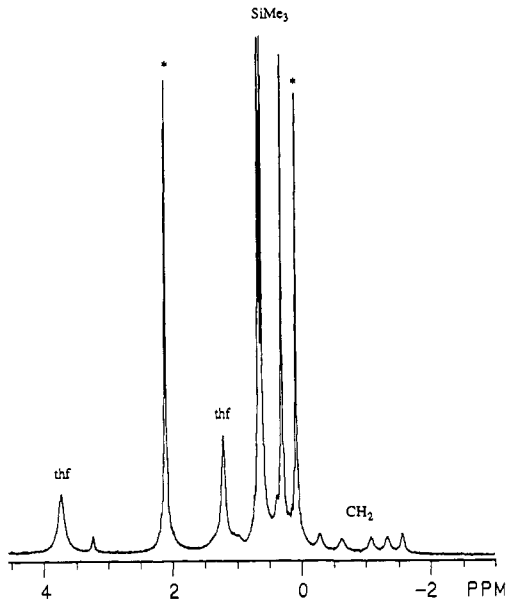

Figure 1. 300-MHz ^1H NMR spectrum of $[Li(thf)_2]_2[Cr_2(CH_2SiMe_3)_6]$ (1) in C_7D_8 at −80 °C. Asterisks indicate peaks due to the solvent and $SiMe_4$.

Results and Discussion

Synthesis and Characterization of the Quadruply Bonded $[Cr_2(CH_2SiMe_3)_6]^{2-}$ Dianion. The addition of three equivalents of [(trimethylsilyl)methyl]lithium to the tetrahydrofuran (thf) adduct of chromium(II) chloride, $CrCl_2(thf)$, yields a brown solution, from which the anionic alkyl complex $[Li(thf)_2]_2[Cr_2(CH_2SiMe_3)_6]$ (1) may be isolated. This dark orange-brown crystalline complex is thermally robust but is air- and moisture-sensitive.

$$2CrCl_2(thf) + 6LiCH_2SiMe_3 + 2thf \rightarrow [Li(thf)_2]_2[Cr_2(CH_2SiMe_3)_6] + 4LiCl$$
1

The NMR spectra of 1 indicate that this molecule is essentially diamagnetic and thus it is probably dimeric with a metal–metal quadruple bond. The ^1H NMR spectrum of 1 at −80 °C in d_8-toluene shows the presence of three equal-intensity $SiMe_3$ resonances near δ 0.5 and five equal-intensity CH_2 resonances between δ 0 and −2 (Figure 1). Evidently, there is a sixth methylene resonances that could not be located (see below). The presence of three different environments for the CH_2SiMe_3 ligands is confirmed by the $^{13}C\{^1H\}$ NMR spectrum at −80 °C, which shows three equal-intensity resonances for the $SiMe_3$ carbons of the (trimethylsilyl)methyl groups (see Figure 2a). Corresponding resonances are also seen for the $SiMe_3$ carbons in the low-temperature solid-state ^{13}C CPMAS NMR spectrum of 1 (Figure 2b).

There are no signals in the solution or solid-state ^{13}C NMR spectra that could be assigned to the methylene carbons of the CH_2SiMe_3 ligands. Magnetic moments measured for other chromium(II) dimers are usually small (<0.9 μ_B) but nonzero and are consistent with a temperature-independent paramagnetic (TIP) effect.[43] Thus, the absence of ^{13}C NMR peaks for the methylene carbons of the CH_2SiMe_3 ligands may be due to broadening of these peaks by paramagnetic relaxation effects.

(43) Larkworthy, L. F.; Tabatabai, J. M. *Inorg. Nucl. Chem. Lett.* **1980**, *16*, 427–431.

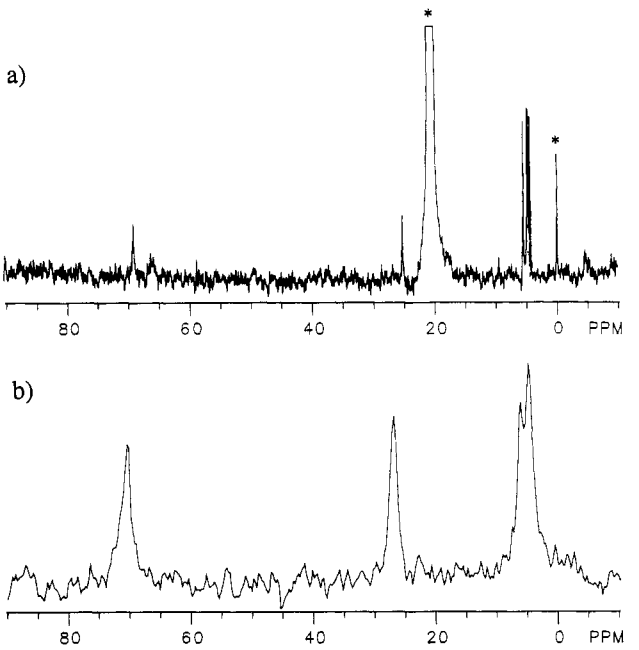

Figure 2. (a) 75.44-MHz solution $^{13}C\{^1H\}$ NMR spectrum of $[Li(thf)_2]_2[Cr_2(CH_2SiMe_3)_6]$ (1) in C_7D_8 at −80 °C. (b) 75.44-MHz solid-state CPMAS ^{13}C NMR spectrum of $[Li(thf)_2]_2[Cr_2(CH_2SiMe_3)_6]$ (1) at −100 °C.

The NMR spectra of the complex are consistent with a quadruply bonded dinuclear structure in which there are two bridging CH_2SiMe_3 groups and two terminal CH_2SiMe_3 ligands on each chromium center. The arrangement of ligands in 1 is probably closely related to that in the electrically neutral dichromium alkyl $Cr_2(CH_2SiMe_3)_4(PMe_3)_2$,[44,45] except that in the latter molecule one alkyl group and one PMe_3 ligand are the terminal substituents on each chromium center (structure III). In $Cr_2(CH_2SiMe_3)_4(PMe_3)_2$, the ligands around each chromium center describe a square plane; the two square planes are joined at an edge and form a dihedral angle of 78°.[45] Accordingly, this molecule has an "A frame" type of structure, and doubtlessly the structure of 1 is similar (structure IV). Presumably, the two $[Li(thf)_2]^+$ cations in 1 are closely associated with the $[Cr_2(CH_2SiMe_3)_6]^{2-}$ dianion, since this salt is appreciably soluble in toluene. Most likely, one

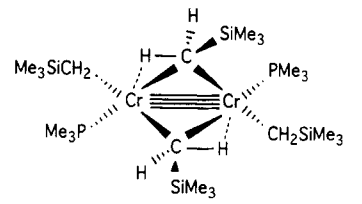

III

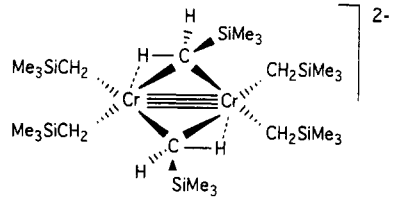

IV

(44) Andersen, R. A.; Jones, R. A.; Wilkinson, G. *J. Chem. Soc., Dalton Trans.* **1978**, 446–453.

(45) Hursthouse, M. B.; Abdul-Malik, K. M.; Sales, K. D. *J. Chem. Soc., Dalton Trans.* **1978**, 1314–1318.

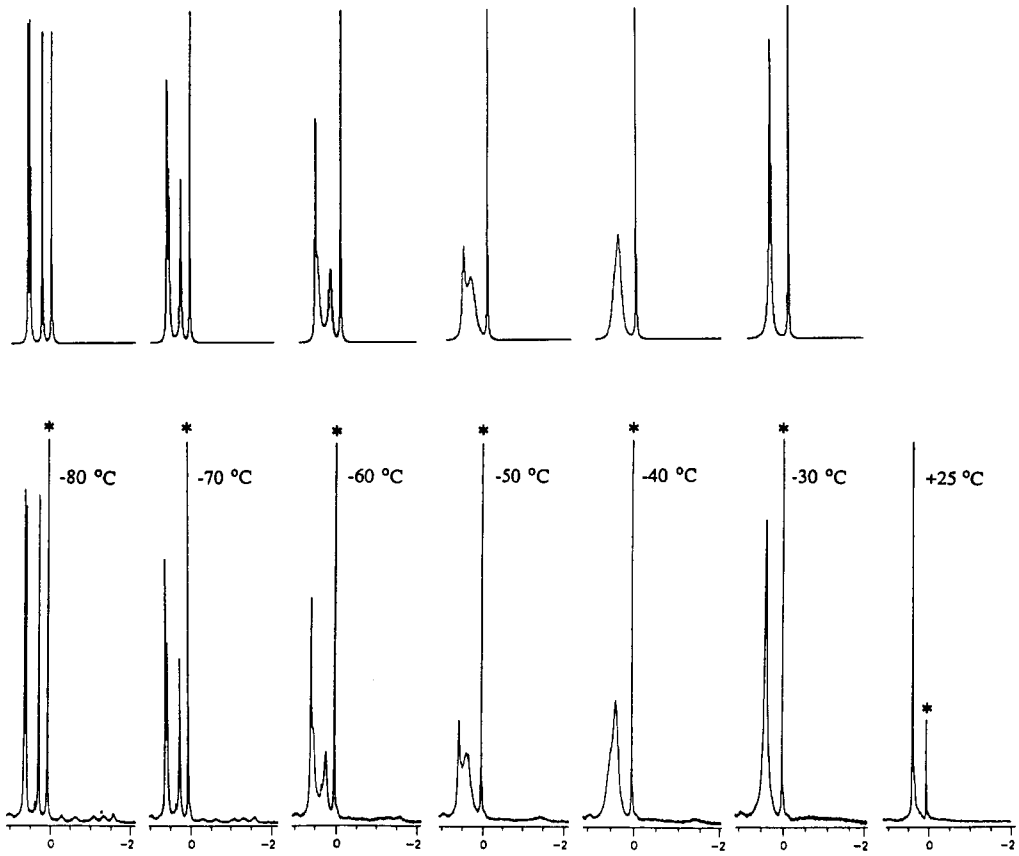

Figure 3. Lower spectra: variable-temperature 300-MHz ^{1}H NMR spectra of $[Li(thf)_2]_2[Cr_2(CH_2SiMe_3)_6]$ (1) in C_7D_8. Asterisks indicate peaks due to $SiMe_4$. Upper spectra: computer-simulated spectra using the rate constants in Table 1. The simulated spectra include the peak for $SiMe_4$ at δ 0; this resonance serves as a useful intensity standard.

$[Li(thf)_2]^+$ cation lies between and interacts with the α-carbon atoms of the two terminal CH_2SiMe_3 ligands on each chromium center, as is often observed in other lithium salts of anionic metal alkyls.[46-49]

The X-ray crystal structure of $Cr_2(CH_2SiMe_3)_4(PMe_3)_2$ clearly shows that one of the two α-hydrogen atoms on each of the bridging CH_2SiMe_3 ligands is involved in an agostic Cr···H–C interaction with a chromium center.[45] Unfortunately, no NMR evidence of this agostic interaction was obtained, since ^{1}H NMR resonances for the α-hydrogen atoms in $Cr_2(CH_2SiMe_3)_4(PMe_3)_2$ could not be located.[44] In contrast, there is clear NMR evidence for such agostic Cr···H–C interactions in 1. Specifically, the presence of three $SiMe_3$ environments and (evidently) six CH_2 environments at −80 °C can only be explained if Cr···H–C interactions involving the bridging (trimethylsilyl)methyl groups are present that lower the symmetry of the molecule from C_{2v} to C_2. Thus, the two terminal CH_2SiMe_3 ligands on each metal center are inequivalent, because one is trans to the Cr···H–C interaction and one is not. If these agostic interactions were not present, one would expect to see only two $SiMe_3$ signals (one resonance each for the bridging and terminal ligands) and three CH_2 signals (one resonance for the bridging ligands and two resonances for the terminal ligands, whose CH_2 protons are diastereotopic).

The presence of an agostic interaction in 1 may also explain why only five of the six methylene proton signals are observable: the sixth agostic hydrogen atom may be selectively broadened by paramagnetic relaxation effects due to its proximity to the chromium center.

Direct evidence of the presence of agostic Cr···H–C interactions in 1 is obtained from its infrared spectrum. The spectrum contains a medium-strong band at 2815 cm^{-1} and a weak absorption at 2690 cm^{-1}; such low-frequency C–H stretching modes are often present in the IR spectra of complexes that possess agostic interactions.[1-3]

Further information about the nature of the Cr···H–C interactions in 1 can be obtained from an analysis of its variable-temperature NMR spectra.

Variable-Temperature Solution and Solid-State NMR Spectra of the $[Cr_2(CH_2SiMe_2)_6]^{2-}$ Dianion. Although at −80 °C the ^{1}H NMR spectrum of 1 contains three resonances for the methyl protons and five resonances for the methylene protons of the CH_2SiMe_3 ligands, at higher temperatures the NMR spectrum changes due to the fluxionality of 1 (Figure 3). As the sample is warmed, the two most shielded (upfield) $SiMe_3$ peaks begin to broaden; by −50 °C these resonances have coalesced to give a broad signal at δ 0.37 whose intensity corresponds to 18 protons. Over the same temperature range the third $SiMe_3$ resonance remains largely unaffected, but at higher temperatures it too broadens, and by +25 °C it has coalesced with the signal of intensity 18 to give a single $SiMe_3$ resonance of intensity 27. The variable-temperature spectra show that the individual CH_2 signals seen at −80 °C also broaden: by −50 °C, some of these peaks have coalesced to give a broad peak at δ −1.45, which further broadens and apparently moves downfield at higher temperatures. By +25 °C, the CH_2 resonance has broad-

(46) Morris, R. J.; Girolami, G. S. *Organometallics* **1989**, *8*, 1478–1485.
(47) Morse, P. M.; Girolami, G. S. *J. Am. Chem. Soc.* **1989**, *111*, 4114–4116.
(48) Morris, R. J.; Girolami, G. S. *Organometallics* **1991**, *10*, 792–799.
(49) Setzer, W. N.; Schleyer, P. v. R. *Adv. Organomet. Chem.* **1985**, *24*, 353–450.

Table 1. Rate Constants for the Dynamic Exchange Processes in 1

temp, K	k_{tt}, s^{-1}	k_{bt}, s^{-1}	temp, K	k_{tt}, s^{-1}	k_{bt}, s^{-1}
203	14	2.8	233	1400	80
213	55	5.5	243	6000[a]	360
223	300	30			

[a] The line shape is essentially invariant for $k_{tt} > 2000$ s^{-1}. The best fit was obtained for $k_{tt} = 6000$ s^{-1}, but this value is very imprecise.

ened to the extent that it is not visible. The signal-to-noise ratios of the methylene signals are too small to permit us to analyze their variable-temperature behavior in any detail; fortunately, however, the $SiMe_3$ resonances can be used to establish the nature of the fluxional processes in which 1 is engaged.

The different rates at which the three $SiMe_3$ peaks broaden as the temperature is raised clearly indicate that 1 undergoes at least *two* fluxional processes. The activation parameters for these dynamic processes can be determined by simulating the variable-temperature line shapes of the $SiMe_3$ resonances. Although there are six $SiMe_3$ groups related in pairs by a C_2 axis in the $[Cr_2(CH_2SiMe_3)_6]^{2-}$ anion, the absence of H–H coupling between these six $SiMe_3$ groups means that the variable-temperature line shapes can be simulated as a three-site problem with site occupancies equal to 1. The chemical shifts of the three exchanging sites were assumed to be temperature-independent. For such a three-site exchange problem, there are three pairwise exchange rates that serve as fitting parameters for the simulations, which we may designate k_{tt}, k_{bt1}, and k_{bt2}, for the rate of exchange of the two terminal CH_2SiMe_3 ligands and for the rates of exchange between the bridging and the two chemically inequivalent terminal CH_2SiMe_3 ligands.

We found that the best fits of the lower temperature spectra were obtained when two of the rate constants were equal. This is a reflection of the fact that the two most shielded (upfield) peaks broaden at the same rate, even over the temperature range where the third peak begins to exchange. On chemical grounds, it is most likely that the two rates that are equal are the bridging/terminal ligand exchange rates (i.e., $k_{bt1} = k_{bt2}$), and this relationship was assumed to hold true at higher temperatures as well, where the line shapes could be fitted with a variety of k_{bt1}/k_{bt2} ratios. Thus, the line shapes were fitted using only two variables, k_{tt} and k_{bt}. The assumption that the two terminal–bridging exchange rates are equal gives us an additional dividend: we can assign the two most shielded $SiMe_3$ peaks in the −80 °C spectrum to the terminal CH_2SiMe_3 ligands and the most deshielded peak (which does not undergo rapid exchange at −50 °C) to the bridging CH_2SiMe_3 ligands.

The best-fit exchange rates as a function of temperature are collected in Table 1; the corresponding simulated spectra very closely match the experimental line shapes (Figure 3). Furthermore, the Eyring plots of $\ln(kh/k_BT)$ vs $1/T$ are reasonably linear for both exchange processes (Figure 4); thus, both processes obey first-order kinetics. The derived activation parameters are $\Delta H^\ddagger = 14.1 \pm 0.6$ kcal mol^{-1} and $\Delta S^\ddagger = 17 \pm 3$ eu for the terminal–terminal ligand exchange process and $\Delta H^\ddagger = 10.6 \pm 0.5$ kcal mol^{-1} and $\Delta S^\ddagger = -4 \pm 2$ eu for the terminal–bridging ligand exchange process. At 273 K, these correspond to activation free energies, $\Delta G^\ddagger$, of 9.5 and 11.7 kcal mol^{-1}, respectively. Interestingly, terminal–terminal ligand exchange, which has the higher activation enthalpy, is the low-temperature exchange process owing to the large positive activation entropy.

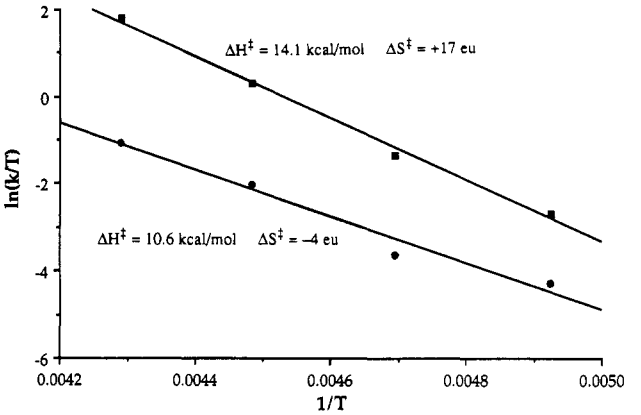

Figure 4. Eyring plots of the rates of rotation of the agostic bridging CH_2SiMe_3 groups in 1 (upper line) and the rates of exchange of the terminal and bridging CH_2SiMe_3 groups in 1 (lower line) as a function of temperature.

Possible Exchange Mechanisms in the $[Cr_2(CH_2SiMe_2)_6]^{2-}$ Dianion. While it is straightforward to measure the activation parameters for the two dynamic processes that 1 undergoes, the assignment of a particular dynamic motion to each process is more problematic. One set of possibilities is discussed below; however, it should be kept in mind that this discussion, like that above, assumes that the most deshielded resonance is due to the bridging alkyl groups (which in turn was based on the assumption that $k_{bt1} = k_{bt2}$). Different conclusions about the exchange mechanisms would necessarily be drawn if this assumption is incorrect.

For the low-temperature process that 1 undergoes, terminal–terminal ligand exchange, the most likely intramolecular mechanism is rotation of the bridging CH_2SiMe_3 ligands about the Cr–C bonds:

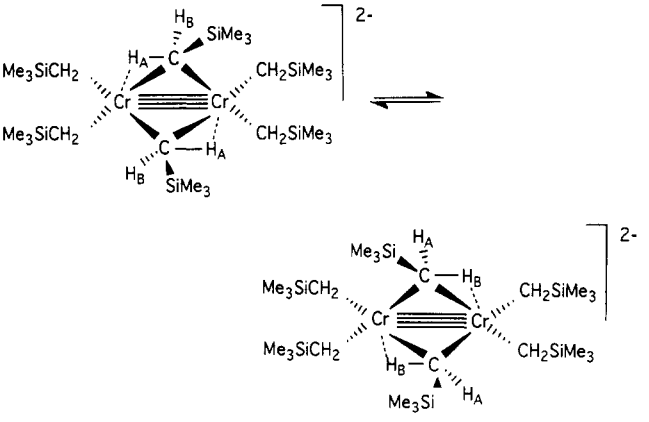

This process exchanges the agostic (H_A) and nonagostic (H_B) hydrogen atoms on each bridging alkyl group; viz., the initially agostic hydrogen atoms become nonagostic and vice versa. This motion would also account for the coalescence of two shielded (terminal) $SiMe_3$ resonances at −50 °C, since the terminal CH_2SiMe_3 ligand trans to the agostic Cr···H–C interaction and the terminal CH_2SiMe_3 ligand cis to this interaction on each chromium center are exchanged. Other dynamic processes that could explain the observed fluxionality, such as the reversible oxidative addition of the agostic C–H bonds to form alkylidene hydride intermediates, seem to us to be less

likely on chemical grounds; the agostic Cr···H bonds are undoubtedly the weakest bonds in the complex and are the most likely to cleave reversibly.

The positive entropy of activation ($\Delta S^{\ddagger} = 17 \pm 3$ eu) for the lower temperature dynamic process in 1 suggests that, during alkyl group rotation, the Cr···H–C agostic interactions are largely broken in the transition state. The activation energy of 9.5 kcal mol^{-1} for exchange of the agostic and nonagostic hydrogen atoms on the bridging alkyl ligands is comparable to those observed in other systems (see Table 2).[16-26,50-71] It is worth pointing out, however, that if rotation of the two bridging CH_2SiMe_3 ligands occurred in a concerted fashion as drawn above, the intrinsic activation energy for a hypothetical single rotation process would be $\Delta G^{\ddagger} = 4.7$ kcal mol^{-1}. Of course, other factors could contribute to the activation parameters, especially steric repulsions involving the $SiMe_3$ groups. Nevertheless, this is only the second molecule in which activation parameters for exchange of agostic and nonagostic α-hydrogen atoms has been determined; in all other cases, molecules that contain such interactions are sufficiently fluxional that a slow-exchange spectrum is not obtainable.

For the higher temperature dynamic process seen in 1, exchange of terminal and bridging CH_2SiMe_3 ligands, the activation entropy is close to zero; one possibility (but by no means the only one) is that exchange of the terminal and bridging alkyl groups is intramolecular and does not involve either dissociation of alkyl groups or bimolecular associative processes. Interestingly, no exchange of the terminal and bridging CH_2SiMe_3 ligands was observed in the phosphine complex $Cr_2(CH_2SiMe_3)_4(PMe_3)_2$, since two separate $SiMe_3$ resonances were observed even at 25 °C.

Table 2. Barriers for Exchange of Agostic and Nonagostic Hydrogen Atoms in Organometallic Complexes

cmpd	$\Delta G^{\ddagger}$, kcal/mol	ref
α-Agostic Interactions		
$Cr_2(CH_2SiMe_3)_4(CHSiMe_3\text{-}\mu\text{-}H)_2^{2-}$	9.5	this work
$Cp_2Ti(\mu\text{-}CH_3)(\mu\text{-}CH_2)Rh(cod)$	9.8	9
$Cp_2Ti(\mu\text{-}CH_3)(\mu\text{-}CH_2)PtMe(PMePh_2)$	*a*	8
β-Agostic Interactions		
$(\eta^3\text{-}C_3H_5)_3Mo(CHMeCH_2\text{-}\mu\text{-}H)$	ca. 8–9	24
$CpW(CO)_2(CH_2CH_2\text{-}\mu\text{-}H)$	10.8	25, 26
$Cp^*Co(L)(CH_2CH_2\text{-}\mu\text{-}H)^+$		
L = C_2H_4	10.3	16
L = P(*p*-tolyl)$_3$	*a*	17
L = PMe_3	10.9	18
L = $P(OMe)_3$	11.1	19
L = PMe_2Ph	9.6	20
$CpCo(L)(CH_2CH_2\text{-}\mu\text{-}H)^+$		
L = PMe_3	12.5	17
L = $P(OMe)_3$	12.5	17
$Cp^*Rh(C_2H_4)(CH_2CH_2\text{-}\mu\text{-}H)^+$	8.5	21
$Ni(t\text{-}Bu_2P(CH_2)_2P\text{-}t\text{-}Bu_2)(CH_2CH_2\text{-}\mu\text{-}H)^+$	*a*	22
$Pd(t\text{-}Bu_2P(CH_2)_3P\text{-}t\text{-}Bu_2)(CH_2CH_2\text{-}\mu\text{-}H)^+$	*a*	22
$Pt(t\text{-}Bu_2P(CH_2)_3P\text{-}t\text{-}Bu_2)(CH_2CH_2\text{-}\mu\text{-}H)^+$	8.0	23
"Remote" Agostic Interactions		
$Cr(CO)_2(L)(\eta^4\text{-}CH_2CMeCHCMeCH_2\text{-}\mu\text{-}H)$		
L = CO	7.9	50
L = $P(OMe)_3$	7.0	51
$Cr(CO)_2(L)(\eta^4\text{-}C_7H_9\text{-}\mu\text{-}H)$		
L = CO	7.0	50, 52
L = $P(OMe)_3$	7.0	50, 52
L = PMe_3	6.7	50, 52
$Cr(PF_3)_3(\eta^4\text{-}C_8H_9\text{-}\mu\text{-}H)$	ca. 10	53
$Mo(CO)_2(\eta^3\text{-}C_3H_5)[B(pz)_2Et(CHMe\text{-}\mu\text{-}H)]$	10.5, ca. 16[b]	54
$Mo(\eta^4\text{-}C_4H_6)(PMe_3)_2(\eta^3\text{-}CH_2CHCHCH_2\text{-}\mu\text{-}H)$	8.9	55
$Mn(CO)_3(\eta^3\text{-}C_6H_8\text{-}\mu\text{-}H)$	8.5	56, 57
$Mn(CO)_3(\eta^3\text{-}C_7H_8\text{-}\mu\text{-}H)$	9.2	58
$Mn(CO)_3(\eta^3\text{-}C_8H_{10}\text{-}\mu\text{-}H)$	<7.8	58
$Mn(CO)_3(\eta^3\text{-}CH_2CHCHCH_2\text{-}\mu\text{-}H)$	9.1	58
$Mn(CO)_3(\eta^3\text{-}CH_2CHCMeCH_2\text{-}\mu\text{-}H)$	8.9	59
$Mn[(Me_2PCH_2)_3CMe](\eta^4\text{-}CH_2CHCHCHCH_2\text{-}\mu\text{-}H)^+$	9.5	60
$Fe(CO)_3(\eta^3\text{-}C_4H_4\text{-}\mu\text{-}H)^+$	*a*	61
$Fe(CO)_3(\eta^3\text{-}CH_2CHCHCH_2\text{-}\mu\text{-}H)^+$	10.2	62–64
$Fe[P(OMe)_3]_3(\eta^3\text{-}CH_2CMeCHCH_2\text{-}\mu\text{-}H)^+$	8.8	65
$Fe(CO)_3(\eta^3\text{-}C_6H_8\text{-}\mu\text{-}H)^+$	11	62–64
$Fe[P(OMe)_3]_3(\eta^3\text{-}C_6H_8\text{-}\mu\text{-}H)^+$	10.0	65
$Fe[P(OMe)_3]_3(\eta^3\text{-}C_7H_{10}\text{-}\mu\text{-}H)^+$	10.5	65
$Fe[P(OMe)_3]_3(\eta^3\text{-}C_8H_{12}\text{-}\mu\text{-}H)^+$	>5	66–68
$Ru(\eta^4\text{-}cod)(\eta^3\text{-}CH_2CHCHCH_2\text{-}\mu\text{-}H)^+$	ca. 20	69
$Ru(\eta^5\text{-}C_5H_5Me_2)(\eta^4\text{-}CH_2CMeCHCMeCH_2\text{-}\mu\text{-}H)^+$	11.4	70
$CpRu(\eta^4\text{-}CH_2CMeCHCMeCH_2\text{-}\mu\text{-}H)^+$	12.5	70
$Cp^*Ru(\eta^4\text{-}CH_2CMeCHCMeCH_2\text{-}\mu\text{-}H)^+$	11.3	70
$Cp^*Rh(\eta^3\text{-}CH_2CMeCMeCH_2\text{-}\mu\text{-}H)^+$	7.5	71

[a] Static at sufficiently low temperatures but no activation data given. [b] Two different dynamic processes are occurring.

This may mean that the $[Li(thf)_2]^+$ cations are involved in the exchange of terminal and bridging CH_2SiMe_3 groups in 1.

We note that recently Gambarotta has synthesized the benzyl analogue of 1, i.e., $[Li(tmed)]_2[Cr_2(CH_2Ph)_6]$. However, no variable-temperature NMR data were reported, although the room-temperature ^1H NMR spectrum suggested that exchange of terminal and bridging benzyl groups must be occurring.[72]

Synthesis and Structure of the Bis(metallacycle) Complex $[Cr(\kappa^2C,C'\text{-}CH_2SiMe_2CH_2)_2]^{2-}$. In an attempt to synthesize other salts of the $[Cr_2(CH_2SiMe_3)_6]^{2-}$ dianion, we added *N,N,N',N'*-tetramethylethylenediamine to a

(50) Kreiter, C. G. *Adv. Organomet. Chem.* **1986**, *26*, 297–375.
(51) Michael, G.; Kaub, J.; Kreiter, C. G. *Angew. Chem., Int. Ed. Engl.* **1985**, *24*, 502–504.
(52) Michael, G.; Kaub, J.; Kreiter, C. G. *Chem. Ber.* **1985**, *118*, 3944–3958.
(53) Blackborrow, J. R.; Iady, C. R.; Gravels, F.-W.; Koerner von Gustorf, E. A.; Scrivanti, A.; Wolfbeis, O. S.; Been, R.; Brauer, D. J.; Kruger, C.; Roberts, P. J.; Tsay, Y.-H. *J. Chem. Soc., Dalton Trans.* **1981**, 661–667.
(54) Cotton, F. A.; Stanislowski, A. G. *J. Am. Chem. Soc.* **1974**, *96*, 5074–5082.
(55) Brookhart, M.; Cox, K.; Cloke, F. G. N.; Green, J. C.; Green, M. L. H.; Hare, P. M. *J. Chem. Soc., Dalton Trans.* **1985**, 423–433.
(56) Lamanna, W.; Brookhart, M. *J. Am. Chem. Soc.* **1981**, *103*, 989–991.
(57) Brookhart, M.; Lamanna, W.; Humphrey, M. B. *J. Am. Chem. Soc.* **1982**, *104*, 2117–2126.
(58) Brookhart, M.; Noh, D. K.; Timmers, F. *Organometallics* **1987**, *6*, 1829–1831.
(59) Timmers, F.; Brookhart, M. *Organometallics* **1985**, *4*, 1365–1371.
(60) Bleeke, J. R.; Kotyk, J. J.; Moore, D. A.; Rauscher, D. J. *J. Am. Chem. Soc.* **1987**, *109*, 417–423.
(61) Olah, G. A.; Liang, G. A.; Yu, S. H. *J. Org. Chem.* **1976**, *41*, 2659–2661.
(62) Young, D. A. T.; Homes, J. R.; Kaesz, H. D. *J. Am. Chem. Soc.* **1969**, *91*, 6968–6977.
(63) Brookhart, M.; Whitesides, T. H.; Crockett, J. M. *Inorg. Chem.* **1976**, *15*, 1550–1554.
(64) Olah, G. A.; Liang, G. A.; Yu, S. H. *J. Org. Chem.* **1976**, *41*, 2227–2228.
(65) Ittel, S. D.; Van-Catledge, F. A.; Jesson, J. P. *J. Am. Chem. Soc.* **1979**, *101*, 6905–6911.
(66) Brown, R. K.; Williams, J. M.; Schultz, A. J.; Stucky, G. D.; Ittel, S. D.; Harlow, R. L. *J. Am. Chem. Soc.* **1980**, *102*, 981–987.
(67) Ittel, S. D.; Van-Catledge, F. A.; Tolman, C. A.; Jesson, J. P. *J. Am. Chem. Soc.* **1978**, *100*, 1317–1318.
(68) Williams, J. M.; Brown, R. K.; Schultz, A. J.; Stucky, G. D.; Ittel, S. D. *J. Am. Chem. Soc.* **1978**, *100*, 7407–7409.
(69) Bennett, M. A.; Wang, X. *J. Organomet. Chem.* **1992**, *428*, C17–C20.
(70) Cox, D. N.; Raymond, R. *J. Chem. Soc., Chem. Commun.* **1989**, 175–176.
(71) Bennett, M. A.; McMahon, I. J.; Pelling, S.; Brookhart, M.; Lincoln, D. M. *Organometallics* **1992**, *11*, 127–138.
(72) Hao, S.; Gambarotta, S., submitted for publication.

Table 3. Crystal Data for $[Li(tmed)]_2[Cr(\kappa^2\text{-}C,C'\text{-}CH_2SiMe_2CH_2)_2]$ (2)

T = −75 °C	space group: $P\bar{1}$
a = 7.811(4) Å	V = 746(2) Å^3
b = 10.336(4) Å	Z = 1
c = 10.720(5) Å	mol wt: 470.71
α = 95.12(3)°	ρ_{calcd} = 1.048 g cm^{-3}
β = 110.87(4)°	μ_{calcd} = 4.64 cm^{-1}
γ = 108.58(5)°	size: 0.1 × 0.4 × 0.7 mm

diffractometer: Enraf-Nonius CAD4
radiation: Mo K$\bar{\alpha}$ ($\bar{\lambda}$ = 0.710 73 Å)
monochromator: graphite crystal, 2θ = 12°
scan range, type: $2.0 < 2\theta < 52.0°$, ω/θ
scan speed, width: 3–16° min^{-1}, $\Delta\omega = 1.50[1.00 + 0.35 \tan\theta]°$
no. of rflns: 3234 total, 2938 unique, 2261 with $I > 2.58\sigma(I)$
internal consistency: R_i = 0.018

R_F = 0.043	variables: 212
R_{wF} = 0.058	p factor: 0.020

solution of $[Li(thf)_2]_2[Cr_2(CH_2SiMe_3)_6]$ in diethyl ether. This action does result in conversion of the $[Li(thf)_2]^+$ cations to $[Li(tmed)]^+$ cations but also promotes γ-hydrogen activation of the CH_2SiMe_3 ligands to give the unique transition-metal bis(metallacycle) complex $[Li(tmed)]_2[Cr(\kappa^2C,C'\text{-}CH_2SiMe_2CH_2)_2]$ (**2**). This complex

$$[Li(thf)_2]_2[Cr_2(CH_2SiMe_3)_6] + 3tmed \rightarrow \underset{\mathbf{2}}{[Li(tmed)]_2[Cr(CH_2SiMe_2CH_2)_2]} + ...$$

$$CrCl_2(thf) + 4LiCH_2SiMe_3 + 3tmed \rightarrow \underset{\mathbf{2}}{[Li(tmed)]_2[Cr(CH_2SiMe_2CH_2)_2]} + ...$$

can also be synthesized directly from $CrCl_2(thf)$ by addition of 4 equiv of $LiCH_2SiMe_3$ and 3 equiv of tmed. Although the mechanism responsible for the formation of **2** has not been established, a balanced reaction can be written if 1 equiv of $Cr(CH_2SiMe_3)_2(tmed)$ and 2 equiv of $SiMe_4$ are generated for every 1 mol of **2** formed. Compound **2** is an orange crystalline compound that is air- and water-sensitive but thermally stable to 180 °C. Its ^1H NMR spectrum shows that the compound is paramagnetic, since a single broad peak (fwhm = 200 Hz) is observed at δ 2.2 for the tmed groups. The other protons in the molecule do not give observable ^1H NMR signals, due presumably to their proximity to the paramagnetic chromium center.

Crystals of $[Li(tmed)]_2[Cr(\kappa^2C,C'\text{-}CH_2SiMe_2CH_2)_2]$ (**2**) crystallize in the triclinic space group $P\bar{1}$, with the one molecule in the unit cell residing on the crystallographic inversion center. Crystal data are presented in Table 3, atomic coordinates are collected in Table 4, and selected bond distances and angles appear in Table 5. The crystallographic results (Figure 5) confirm that **2** is in fact a bis(metallacycle) complex with two bidentate 2,2-dimethyl-2-silapropane-1,3-diyl groups. The chromium atom is in a square-planar environment, as is common for high-spin d^4 chromium(II) centers;[73] in this case, the crystallographic inversion symmetry guarantees that the four α-carbon atoms and the chromium center are mutually co-planar.

The average Cr–C distance in $[Li(tmed)]_2[Cr(\kappa^2C,C'\text{-}CH_2SiMe_2CH_2)_2]$ of 2.235(5) Å is some 0.1 Å longer than typical Cr–C distances in electrically neutral chromium(II) alkyl complexes: 2.128(4) Å in $Cr(CH_2CMe_3)_2(dippe)$,[73] 2.149(8) Å in $Cr(CH_2SiMe_3)_2(dippe)$,[73] 2.131(2) Å in

(73) Hermes, A. R.; Morris, R. J.; Girolami, G. S. *Organometallics* **1988**, *7*, 2372–2379.

Table 4. Atomic Coordinates for $[Li(tmed)]_2[Cr(\kappa^2C,C'\text{-}CH_2SiMe_2CH_2)_2]$ (2)

	x/a	y/b	z/c
Cr	0.0	0.0	0.0
Si	0.2441(1)	0.21797(8)	0.23753(8)
C(7)	0.2664(5)	0.1981(3)	0.0727(3)
C(8)	0.0854(5)	0.0399(3)	0.2268(3)
C(9)	0.4895(5)	0.2893(4)	0.3903(3)
C(10)	0.1181(7)	0.3414(5)	0.2501(5)
Li	0.1819(7)	0.1497(5)	−0.1460(5)
N(1)	0.1533(4)	0.3076(3)	−0.2618(3)
N(2)	0.4295(4)	0.1606(3)	−0.1968(3)
C(1)	0.2845(6)	0.3088(4)	−0.3320(4)
C(2)	0.4667(6)	0.2918(5)	−0.2449(4)
C(3)	−0.0454(6)	0.2794(5)	−0.3652(4)
C(4)	0.2182(7)	0.4440(4)	−0.1721(4)
C(5)	0.6138(6)	0.1787(5)	−0.0801(4)
C(6)	0.3768(7)	0.0412(5)	−0.3026(6)
H(1a)	0.215(4)	0.210(4)	−0.415(4)
H(1b)	0.338(4)	0.407(4)	−0.356(3)
H(2a)	0.543(4)	0.283(4)	−0.308(3)
H(2b)	0.517(4)	0.384(4)	−0.168(4)
H(3a)	−0.065(4)	0.193(4)	−0.423(4)
H(3b)	−0.042(4)	0.344(4)	−0.425(4)
H(3c)	−0.136(4)	0.263(4)	−0.309(4)
H(4a)	0.381(4)	0.482(4)	−0.095(4)
H(4b)	0.210(4)	0.528(4)	−0.221(4)
H(4c)	0.126(5)	0.444(4)	−0.126(4)
H(5a)	0.646(4)	0.246(4)	−0.006(4)
H(5b)	0.601(4)	0.099(4)	−0.051(4)
H(5c)	0.728(5)	0.203(4)	−0.107(4)
H(6a)	0.472(5)	0.026(4)	−0.318(4)
H(6b)	0.246(5)	0.032(4)	−0.387(4)
H(6c)	0.370(4)	−0.038(4)	−0.252(4)
H(7a)	0.307(4)	0.288(2)	0.051(3)
H(7b)	0.367(3)	0.166(3)	0.067(4)
H(8a)	0.022(4)	0.048(4)	0.287(2)
H(8b)	0.158(4)	−0.017(3)	0.264(3)
H(9a)	0.005(5)	0.315(4)	0.177(4)
H(9b)	0.109(4)	0.357(4)	0.335(4)
H(9c)	0.199(4)	0.436(4)	0.254(4)
H(10a)	0.513(4)	0.329(4)	0.482(4)
H(10b)	0.595(5)	0.366(4)	0.395(4)
H(10c)	0.539(5)	0.227(4)	0.396(4)

Table 5. Selected Bond Distances (Å) and Angles (deg) for $[Li(tmed)]_2[Cr(\kappa^2C,C'\text{-}CH_2SiMe_2CH_2)_2]$ (2)

Bond Distances			
Cr–C(7)	2.230(3)	Cr···Si	2.824(1)
Cr–C(8)	2.240(3)	Cr···Li	2.734(5)
Si–C(7)	1.836(3)	Li···H(7a)	2.13(3)
Si–C(8)	1.829(3)	Li···H(7b)	2.18(3)
Si–C(9)	1.883(3)	Li···H(8a)	2.16(3)
Si–C(10)	1.864(5)	Li···H(8b)	2.35(3)
Li–N(1)	2.158(6)	C(7)–H(7a)	0.96[b]
Li–N(2)	2.161(6)	C(7)–H(7b)	0.96[b]
Li–C(7)	2.158(6)	C(8)–H(8a)	0.96[b]
Li–C(8)	2.179(6)	C(8)–H(8b)	0.96[b]
C(1)–C(2)	1.473(6)		

Bond Angles			
C(7)–Cr–C(7)′	180.0[a]	Cr–C(7)–H(7a)	139(2)
C(8)–Cr–C(8)′	180.0[a]	Cr–C(7)–H(7b)	103(2)
C(7)–Cr–C(8)	79.0(1)	Cr–C(8)–H(8a)	136(2)
C(7)–Cr–C(8)′	101.0(1)	Cr–C(8)–H(8b)	108(2)
C(7)–Si–C(8)	101.7(1)	H(7a)–C(7)–H(7b)	101(3)
C(9)–Si–C(10)	106.3(2)	H(8a)–C(8)–H(8b)	104(3)
Cr–C(7)–Si	87.4(1)	Li–C(7)–H(7a)	76(2)
Cr–C(8)–Si	87.3(1)	Li–C(7)–H(7b)	78(2)
Cr–C(7)–Li	77.0(2)	Li–C(8)–H(8a)	76(2)
Cr–C(8)–Li	76.4(2)	Li–C(8)–H(8b)	88(2)
Si–C(7)–Li	159.9(2)	Si–C(7)–H(7a)	110(2)
Si–C(8)–Li	156.8(2)	Si–C(7)–H(7b)	118(2)
C(7)–Li–C(8)	105.4(2)	Si–C(8)–H(8a)	107(2)
N(1)–Li–N(2)	85.9(2)	Si–C(8)–H(8b)	113(2)

[a] Crystallographically imposed. [b] Constrained value.

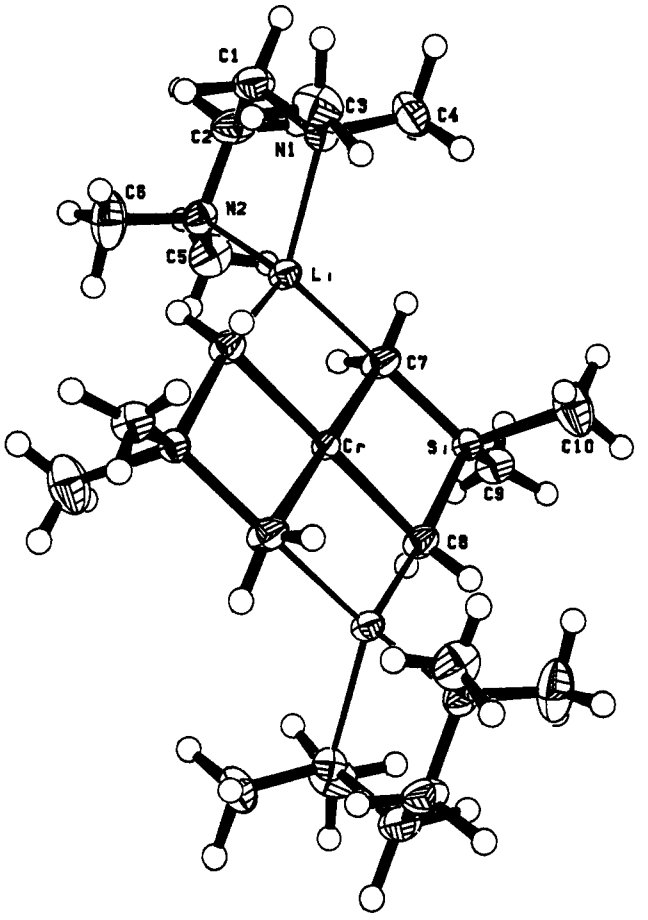

Figure 5. Molecular structure of $[Li(tmed)]_2[Cr(\kappa^2C,C'\text{-}CH_2SiMe_2CH_2)_2]$ (**2**). Thermal ellipsoids represent the 35% probability density surfaces.

$Cr_2(CH_2SiMe_3)_4(PMe_3)_2$,[45] 2.168(4) Å in $CrMe_2(dmpe)_2$,[74] and 2.22(1) Å in $Cr_2[(CH_2)_2PMe_2]_4$.[75] However, anionic chromium(II) alkyls generally have longer Cr–C distances that are more similar to those in compound **2**: 2.20(1) Å in $[Li(thf)]_4[Cr_2Me_8]$,[76] 2.24(3) Å in $[Li(OEt_2)]_4[Cr_2(C_4H_8)_4]$,[77] and 2.209(4) Å in $[Li(tmed)]_2[CrMe_4]$.[78]

The metric parameters of the metallacyclic rings in **2** are generally similar to those of other metallacyclobutane complexes of the early transition elements.[79–83] Particularly instructive is a comparison with the structures of $Cp_2M(CH_2SiMe_2CH_2)$ for M = Zr, Nb, and Mo. In this series of molecules, the C–M–C angle decreases from 81 to 72°, the C–Si–C angle decreases from 102 to 96°, and the fold angle of the ring increases from 5 to 14° as the number of d electrons increases from 0 to 2.[79] These changes were attributed to population of a metal–ligand antibonding orbital in the niobium and molybdenum complexes. In **2**, the corresponding angles (C–M–C = 79.0(1)°, C–Si–C = 101.7(1)°, and a fold angle of 23.7°) most closely resemble that of the d^0 zirconocene complex, except that the ring in **2** is significantly more puckered. The silicon atoms in **2** lie 0.465(1) Å out of the CrC_4 plane.

The lithium atoms bridge between the metallacyclic rings via interactions with the α-methylene groups; each lithium atom completes its tetrahedral coordination sphere by binding a tmed ligand. The lithium atoms lie only 0.068(5) Å from the CrC_4 plane and thus complete a "windowpane" type structure for the molecule as a whole that consists of four fused coplanar four-membered rings. The average carbon–lithium contact distance of 2.168(6) Å in **2** is well within the 2.60-Å sum of the van der Waals radii of a methyl group and a lithium atom. The 2.168-Å distance is somewhat shorter than the typical C–Li contact distances of 2.23–2.27 Å for alkyllithium reagents and the average C–Li distances of 2.37(3) Å in $[Li(thf)]_4[Cr_2Me_8]$[76] and 2.39(7) Å in $[Li(OEt_2)]_4[Cr_2(C_4H_8)_4]$[77] but is comparable to the 2.176(7) Å distance in $[Li(tmed)]_2[CrMe_4]$.[78] The nature of the interactions between lithium cations and alkylmetalate anions has been discussed elsewhere in detail;[46] the principal conclusion, that the primary interaction is between lithium and carbon (and not between lithium and hydrogen), also holds in the present case.

The hydrogen atoms surfaced in the difference Fourier maps, and their positions were refined. Although the C–H distances to the α-methylene hydrogen atoms were constrained, some comments concerning the dispositions of the hydrogen atoms are appropriate. The methylene carbon atoms bound to the chromium center are five-coordinate and possess distorted-trigonal-bipyramidal geometries. The silicon and lithium atoms occupy the axial positions of the distorted trigonal bipyramid, and the "trans" Li···C–Si angle averages 158.3°. Interestingly, the Cr–C–H angles are not all identical: on each CH_2 group, one of the Cr–C–H angles is near the expected tetrahedral value, 103(2)°, but the other is much larger than usual, 139(2)°. A similar distortion of metal-bound alkyl groups due to interactions with nearby lithium atoms has been seen in the manganese ethyl complex $[Li(tmed)]_2[MnEt_4]$.[46]

Gambarotta has recently reported the synthesis and structure of a chromium(II) metallacycle prepared in a fashion similar to our synthesis of **2**, the neopentyl-derived complex $[Li(tmed)]_2[Cr(\kappa^2C,C'\text{-}CH_2CMe_2CH_2)(CH_2CMe_3)_2]$.[72] Interestingly, in this compound, only one metallacyclobutane ring is generated by γ-hydrogen elimination under the reaction conditions employed.

Concluding Remarks. We have isolated two different chromium(II) alkyl complexes from the alkylation of $CrCl_2$ with [(trimethylsilyl)methyl]lithium, $LiCH_2SiMe_3$. Notably, the complex isolated is dictated by the choice of the Lewis base used to coordinate to the lithium counterions: the quadruply bonded dimer $[Cr_2(CH_2SiMe_3)_6]^{2-}$ if the Lewis base is tetrahydrofuran, and the unusual monomeric bis(metallacycle) complex $[Cr(\kappa^2C,C'\text{-}CH_2SiMe_2CH_2)_2]^{2-}$ if the Lewis base is *N,N,N',N'*-tetramethylethylenediamine. The ability of the counterion to influence the nuclearity of the chromium(II) species isolated has been observed previously in the chromium(II) permethyl complexes $[Li(thf)_2]_4[Cr_2Me_8]$ vs $[Li(tmed)]_2[CrMe_4]$.[78]

Perhaps the most interesting result we have obtained is the determination of the activation parameters for

(74) Girolami, G. S.; Wilkinson, G.; Galas, A. M. R.; Thornton-Pett, M.; Hursthouse, M. B. *J. Chem. Soc., Dalton Trans.* **1985**, 1339–1348.
(75) Cotton, F. A.; Hanson, B. E.; Ilsley, W. H.; Rice, G. W. *Inorg. Chem.* **1979**, *18*, 2713–2717.
(76) Krause, J.; Marx, G.; Schödl, G. *J. Organomet. Chem.* **1970**, *21*, 159–168.
(77) Krause, J.; Schödl, G. *J. Organomet. Chem.* **1971**, *27*, 59–67.
(78) Hao, S.; Gambarotta, S.; Bensimon, C. *J. Am. Chem. Soc.* **1992**, *114*, 3556–3557.
(79) Tikkanen, W. R.; Liu, J. Z.; Egan, J. W., Jr.; Petersen, J. L. *Organometallics* **1984**, *3*, 825–830.
(80) Tikkanen, W. R.; Egan, J. W., Jr.; Petersen, J. L. *Organometallics* **1984**, *3*, 1646–1650.
(81) Kabi-Satpathy, A.; Bajgur, C. S.; Reddy, K. P.; Petersen, J. L. *J. Organomet. Chem.* **1989**, *364*, 105–117.
(82) Bruno, J. W.; Marks, T. J.; Day, V. W. *J. Am. Chem. Soc.* **1982**, *104*, 7357–7360.
(83) Cilberto, E.; Di Bella, S.; Gulino, A.; Fragala, I.; Petersen, J. L.; Marks, T. J. *Organometallics* **1992**, *11*, 1727–1737.

exchange of agostic and nonagostic α-hydrogen atoms in a transition-metal alkyl complex. The activation entropy suggests that the exchange process involves cleavage of the agostic M···H–C interaction before the new M···H–C bond is formed. If one assumes that bond-breaking processes are the the predominant contributors to the activation enthalpy, and that two agostic interactions are broken in the transition state, then the bond dissociation energy involved in breaking a single agostic interaction in this complex is 4.7 kcal mol^{-1}. This may be compared with the only other such measurement reported to date, the 9.8 kcal mol^{-1} value determined for $Cp_2Ti(\mu\text{-}CH_3)(\mu\text{-}CH_2)Rh(cod)$.

Experimental Section

All operations were conducted under vacuum or under argon. Diethyl ether and tetrahydrofuran were distilled from sodium–benzophenone immediately before use. *N,N,N′,N′*-Tetramethylethylenediamine (Aldrich) was purified by distillation from sodium. [(Trimethylsilyl)methyl]lithium[84] and $CrCl_2(thf)$[85] were prepared by following literature routes.

Microanalyses were performed by the University of Illinois Microanalytical Laboratory. The IR spectra were recorded on a Perkin-Elmer 599B instrument as Nujol mulls between KBr plates. The solution NMR data were recorded on a General Electric QE-300 instrument or on a General Electric GN-300 NB instrument at 300 MHz (^1H) or 75.44 MHz (^{13}C). The solid-state NMR data were recorded on a General Electric GN-300 WB instrument at 75.44 MHz (^{13}C) by using the cross-polarized magic angle spinning (CPMAS) technique. Chemical shifts are reported in δ units (positive chemical shifts to higher frequency) relative to $SiMe_4$. Melting points were recorded on a Thomas-Hoover Unimelt apparatus in closed capillaries under argon.

Simulations of the dynamic NMR spectra were carried out using the program DNMR, which is available from the Quantum Chemistry Program Exchange. The rates of exchange as a function of temperature were determined from visual comparisons of experimental spectra with computed trial line shapes. The errors in the rate constants of ca. 5% were estimated on the basis of subjective judgments of the sensitivities of the fits to changes in the rate constants. The temperature of the NMR probe was calibrated using a methanol temperature standard, and the estimated error in the temperature measurements was 1 K. The activation parameters were calculated from an unweighted nonlinear least-squares procedure contained in the program Passage, which is available from Passage Software Inc. The errors in the activation parameters were computed from the following error propagation formulas, which were derived from the Eyring equation:[86]

$$(\sigma\Delta H^{\ddagger})^2 = \frac{R^2 T_{max}^{\ 2} T_{min}^{\ 2}}{\Delta T^2}\left\{\left(\frac{\sigma T}{T}\right)^2\left[\left(1 + T_{min}\frac{\Delta L}{\Delta T}\right)^2 + \left(1 + T_{max}\frac{\Delta L}{\Delta T}\right)^2\right] + 2\left(\frac{\sigma k}{k}\right)^2\right\}$$

$$(\sigma\Delta S^{\ddagger})^2 = \frac{R^2}{\Delta T^2}\left\{\left(\frac{\sigma T}{T}\right)^2\left[T_{max}^{\ 2}\left(1 + T_{min}\frac{\Delta L}{\Delta T}\right)^2 + T_{min}^{\ 2}\left(1 + T_{max}\frac{\Delta L}{\Delta T}\right)^2\right] + \left(\frac{\sigma k}{k}\right)^2(T_{max}^{\ 2} + T_{min}^{\ 2})\right\}$$

where $\Delta T = (T_{max} - T_{min})$ and $\Delta L = [\ln(k_{max}/T_{max}) - \ln(k_{min}/T_{min})]$.

Bis[bis(tetrahydrofuran)lithium] Hexakis[(trimethylsilyl)methyl]dichromate(II) (1). To a slurry of $CrCl_2(thf)$ (0.45 g, 2.3 mmol) in diethyl ether (60 mL) at 0 °C was added [(trimethylsilyl)methyl]lithium (14.9 mL of a 0.48 M solution in diethyl ether, 7.1 mmol). The solution turned brown immediately and after being stirred for 30 min was warmed to room temperature. The solution was stirred for an additional 4 h and then was filtered, concentrated to ca. 20 mL, and cooled to −20 °C to yield brown crystals. Yield: 0.26 g (16%). Mp: 133 °C dec. Anal. Calcd for $C_{32}H_{82}Cr_2Li_2O_2Si_6$: C, 49.0; H, 10.6; Li, 1.8; Cr, 11.8. Found: C, 46.8; H, 10.5; Li, 1.9; Cr, 11.8. ^1H NMR (C_7D_8, 20 °C): δ 0.34 (s, $SiMe_3$), 1.43 (s, OCH_2CH_2), 3.74 (s, OCH_2). $^{13}C\{^1H\}$ NMR (C_7D_8, −80 °C): δ 4.7 (s, $SiMe_3$), 4.8 (s, $SiMe_3$), 5.5 (s, $SiMe_3$), 25.3 (s, OCH_2CH_2), 68.0 (s, OCH_2). ^{13}C CPMAS NMR (solid, −100 °C): δ 5.1 (s, $SiMe_3$), 6.4 (s, $SiMe_3$), 27.1 (s, OCH_2CH_2), 70.5 (s, OCH_2). IR (cm^{-1}): 2760 w, 1910 w, 1780 w, 1341 w, 1245 s, 1190 w, 1095 w, 1032 s, 932 m, 890 s, 852 s, 822 s, 740 s, 678 s, 608 w, 588 m, 516 m, 462 m, 418 w.

Bis[(*N,N,N′,N′*-tetramethylethylenediamine)lithium] Bis(2-methyl-2-silapropane-1,3-diyl)chromate(II) (2). To a suspension of $CrCl_2(thf)$ (0.53 g, 2.7 mmol) in diethyl ether (60 mL) at 0 °C was added [(trimethylsilyl)methyl]lithium (17.6 mL of a 0.48 M solution in diethyl ether, 8.4 mmol). The solution turned brown immediately, and a white solid precipitated. The solution was stirred for 15 min, and *N,N,N′,N′*-tetramethylethylenediamine (0.73 mL, 5.4 mmol) was added. The solution was warmed to room temperature and was stirred for 3 h. The solution was filtered, concentrated to ca. 40 mL, and cooled to −20 °C to yield orange crystals. A second crop of crystals can be obtained by concentration and cooling of the supernatant. Yield: 0.48 g (34%). Mp: 180 °C dec. Anal. Calcd for $C_{16}H_{52}CrLi_2N_4Si_2$: C, 51.1; H, 11.2; N, 11.9; Li, 3.0; Cr, 11.1. Found: C, 49.5; H, 11.1; N, 11.7; Li, 3.2; Cr, 11.7. ^1H NMR (C_6D_6, 20 °C): δ 2.2 (br s, NMe_2, fwhm = 200 Hz). IR (cm^{-1}): 2795 w, 1356 m, 1322 w, 1289 s, 1250 m, 1225 s, 1177 w, 1155 m, 1128 m, 1095 w, 1068 m, 1034 s, 1021 s, 950 s, 913 m, 829 s, 789 s, 745 s, 723 s, 698 s, 658 m, 615 w, 584 w, 533 m.

Crystallographic Studies.[87] Single crystals of $[Li(tmed)]_2[Cr(\kappa^2CC'\text{-}CH_2SiMe_2CH_2)_2]$ (2), grown from diethyl ether, were mounted on glass fibers with Paratone-N oil (Exxon) and immediately cooled to −75 °C under a nitrogen stream on the diffractometer. Preliminary photographs yielded rough cell dimensions, and standard peak search and automatic indexing procedures, followed by least-squares refinement using 25 reflections, yielded the cell dimensions given in Table 3.

Data were collected in two quadrants of reciprocal space $(-h,\pm k,\pm l)$ using measurement parameters listed in Table 3. The triclinic Laue symmetry was consistent with space groups $P1$ and $P\bar{1}$, and the average values of the normalized structure factors suggested the centric choice $P\bar{1}$, which was confirmed by successful refinement of the proposed model. The measured intensities were reduced to structure factor amplitudes and their esd's by correction for background, scan speed, and Lorentz and polarization effects. While corrections for crystal decay were unnecessary, absorption corrections were applied, the maximum and minimum transmission factors being 0.956 and 0.845, respectively. Symmetry-equivalent reflections were averaged to yield the set of unique data. Only those data with $I > 2.58\sigma(I)$ were used in the least-squares refinement.

The structure was solved using Patterson (SHELXS-86) and weighted difference Fourier methods. The positions of the chromium and silicon atoms were deduced from a vector map, and subsequent difference Fourier calculations revealed the positions of the remaining non-hydrogen atoms. The quantity minimized by the least-squares program was $\sum w(|F_o| - |F_c|)^2$, where $w = 2.08/(\sigma(F_o)^2 + (pF_o)^2)$. The analytical approximations to the scattering factors were used, and all structure factors were corrected for both the real and imaginary components of

(84) Lewis, H. L.; Brown, T. L. *J. Am. Chem. Soc.* **1970**, *92*, 4664–4670.
(85) Larkworthy, L. F.; Nelson-Richardson, M. H. O. *Chem. Ind. (London)* **1974**, 164–165.
(86) These formulas are different from those derived from the Arrhenius equation. See: Steigel, A.; Sauer, J.; Kleier, D. A.; Binsch, G. *J. Am. Chem. Soc.* **1972**, *94*, 2770–2779.
(87) For further details of the crystallographic programs and refinements used, see: Jensen, J. A.; Wilson, S. R.; Girolami, G. S. *J. Am. Chem. Soc.* **1988**, *110*, 4977–4982.

anomalous dispersion. Hydrogen atoms were located in the Fourier difference maps, and their locations were independently refined except for hydrogen atoms H7a through H8b, which were refined with a common C–H bond distance constrained to 0.96(1) Å. In the final cycle of least squares, all non-hydrogen atoms were independently refined with anisotropic thermal coefficients, and a group isotropic thermal parameter was also varied for the hydrogen atoms. Successful convergence was indicated by the maximum shift/error of 0.033 in the last cycle. Final refinement parameters are given in Table 3. The largest peaks in the final difference Fourier map (+0.54 e/Å^3) were located in the vicinity of the tmed ligand, possibly indicating a slight disorder for atoms C1 and C2. A final analysis of variance between observed and calculated structure factors showed a slight inverse dependence on sin θ.

Acknowledgment. We thank the National Science Foundation (Grant CHE 89-17586) and the Union Carbide Innovation Recognition Program for support of this research. M.D.S. acknowledges receipt of a fellowship from the Department of Chemistry at the University of Illinois. We thank Professor W. G. Klemperer for providing a copy of the DNMR program and instructions for its use and Professor S. Gambarotta for sharing his results with us prior to publication. We also thank Charlotte Stern of the University of Illinois X-ray Diffraction Laboratory for assistance with the X-ray crystal structure determination. G.S.G. is the recipient of an A. P. Sloan Foundation Research Fellowship (1988–1993) and a Henry and Camille Dreyfus Teacher–Scholar Award (1988–1993).

Supplementary Material Available: Tables of thermal parameters and bond distances and angles for [Li(tmed)]$_2$[Cr(κ^2C,C'-$CH_2SiMe_2CH_2)_2$] (2 pages). Ordering information is given on any current masthead page.

OM9308351